Modeling of resin transfer molding of composite materials with oriented unidirectional plies
by Dell Raymond Humbert

A thesis submitted in partial fulfillment of the requirements for the degree of Master of Science in Chemical Engineering
Montana State University


Abstract:
The goal of this research was to develop a computer model for the treatment of Resin Transfer Molding (RTM) of unidirectional layer stranded fabrics oriented in various directions. The individual fabric layers contain high fiber volume fraction strands, separated by channels, which the model includes as separate phases. A finite difference approximation has been developed to determine the effective permeability of the channels. This approximation is based on classical channel flow equations, and is applied to all three directions of the channels. The axial permeability in the strands has been measured. The transverse permeabilities in the strands are assumed to be equal, and are fitted to the model results.

The model consists of a finite difference routine which uses cell centered grids to approximate the geometry of the reinforcement. The moving boundary resin is treated as a constant pressure condition. The injection and vent ports are also modeled as constant pressure conditions.

The model has been correlated with experimental results. Simulations and experiments have been run using a single fabric layer at 0°, two layers at ±45°, and three layers at 45°/0°/-45° and 0/±45°. The model accurately captures the flow front shape for each case, and shows general agreement with the positions vs. time.

# MODELING OF RESIN TRANSFER MOLDING OF COMPOSITE MATERIALS WITH ORIENTED UNIDIRECTIONAL PLIES

By

Dell Raymond Humbert

A thesis submitted in partial fulfillment
of the requirements for the degree

of

Master of Science

in

Chemical Engineering

MONTANA STATE UNIVERSITY---BOZEMAN
Bozeman, Montana

April 1996

APPROVAL

of a thesis submitted by

Dell R. Humbert

This thesis has been read by each member of the thesis committee and has been found to be satisfactory regarding content, English usage, format, citations, bibliographic style, and consistency, and is ready for submission to the College of Graduate Studies.

4/23/96 — Date
John J. Mandel — Chairman, Graduate Committee

Approved for the Major Department

4/23/96 — Date
John T. Sears — Head, Major Department

Approved for the College of Graduate Studies

4/25/96 — Date
R L Brown — Graduate Dean

## STATEMENT OF PERMISSION TO USE

In presenting this thesis in partial fulfillment of the requirements for a master's degree at Montana State University, I agree that the library shall make it available to borrowers under the rules of the library.

If I indicated my intention to copyright this thesis by including a copyright notice page, copying is allowable only for scholarly purposes, consistent with "fair use" as prescribed in the U.S. Copyright Law. Requests for permission for extended quotation from or reproduction of this thesis in whole or in parts may be granted only by the copyright holder.

Signature

4/23/96

Date

# ACKNOWLEDGMENTS

This work was supported through the Montana DOE EPSCoR Wind Energy Program DE-FCO2-91ER75681. Their Support is Greatfully Acknowledged.
Many thanks to Dr. Mandell for support, and direction.
Also thanks to Harry, Betty, Chuck, and Dan.

# TABLE OF CONTENTS

TABLE OF CONTENTS -- Continued

# LIST OF TABLES

# LIST OF FIGURES

LIST OF FIGURES—Continued

MODELING OF RESIN TRANSFER MOLDING OF COMPOSITE MATERIALS
WITH ORIENTED UNIDIRECTIONAL PLIES

Dell Raymond Humbert, 1996

## ABSTRACT

The goal of this research was to develop a computer model for the treatment of Resin Transfer Molding (RTM) of unidirectional layer stranded fabrics oriented in various directions. The individual fabric layers contain high fiber volume fraction strands, separated by channels, which the model includes as separate phases. A finite difference approximation has been developed to determine the effective permeability of the channels. This approximation is based on classical channel flow equations, and is applied to all three directions of the channels. The axial permeability in the strands has been measured. The transverse permeabilities in the strands are assumed to be equal, and are fitted to the model results.

The model consists of a finite difference routine which uses cell centered grids to approximate the geometry of the reinforcement. The moving boundary resin is treated as a constant pressure condition. The injection and vent ports are also modeled as constant pressure conditions.

The model has been correlated with experimental results. Simulations and experiments have been run using a single fabric layer at 0°, two layers at ±45°, and three layers at 45°/0°/-45° and 0/±45°. The model accurately captures the flow front shape for each case, and shows general agreement with the positions vs. time.

# CHAPTER ONE

# INTRODUCTION

Polymer matrix composites are very strong and light weight materials. These materials consist of many strong fibers surrounded by a polymer matrix. The fibers provide the strength and stiffness to the material, and the matrix holds the fibers in place and transfers internal loads between them. The matrix also protects the fibers from environmental damage. The fiber properties, content, orientation and arrangement determine the strength of the composite. Composites are now finding application in products ranging from computer main boards and automobile parts, to high performance athletic equipment such as skis and bicycles.

As composite material applications have increased in breadth, a demand for new, low cost, high-quality fabrication techniques has also developed. Current techniques for manufacturing composites include prepreg molding, pultrusion, resin transfer molding, filament winding, compression molding, and hand lay-up. These methods represent a broad spectrum in terms of product expense and quality. Resin Transfer Molding (RTM) has shown promise in its ability to produce high quality products at a relatively low cost. It also has advantages in decreased volatiles emissions and geometric flexibility. Historically, this method has increased in popularity as lower viscosity resins have been developed, since the resin flow requirements are more demanding than with other processing methods.

Resin Transfer Molding involves placing oriented fiber preforms into a mold. The mold is then closed, and resin is injected into the mold cavity. Air is vented from the mold at strategic points during resin injection. The resin is allowed to cure, and the part is removed. The part may then be post cured in an oven to complete the resin cure.

Fiber preforms in structural parts typically consist of many layers of fibers, each in the form of stitched fabrics containing strands of hundreds or thousands of individual fibers. Each layer can have a different fiber orientation. Since the layers have strong properties in only one direction (parallel to the fibers), these differing orientations produce a finished product which is strong in the required directions only, saving material when compared with randomly oriented fibers. The materials of which these layers are made can consist of anything from woven fabric to unidirectional stitched fabrics, and random fiber mats. This variability of reinforcement types, and their complex interlayer interactions, provide a rich variety of resin flow patterns during fabrication. These interlayer flow patterns can make the difference between a mold design which works well, and one which produces flawed parts.

The increasing use of RTM in the production of high performance composite materials has sparked interest in the modelling of these processes. Of great interest is the ability to predict the flow patterns and pressures required for the production of complex geometries. The flow patterns allow the accurate placement of injection and vent ports. If these ports are placed inaccurately, the mold may fill incompletely, resulting in part rejection and inefficient use of both time and materials.

Two approaches to modeling RTM prevail in the literature. The first assumes that the fabric is a homogeneous, anisotropic medium; which has limitations when the principal permeabilities of the plies cannot be captured in al overall approach. The second approach assumes a regular fiber packing and models fluid flow around individual fibers. A model based on such fine detail would be prohibitively complex and time consuming to implement in an algorithm. The present approach is an attempt at combining these two methods. The micro flow regime is taken into account by application of Darcy's law to the bundles, and by calculating an equivalent permeability from the geometry of the channels. This approach leads to a view of the process which will maintain most of the microflow characteristics, while remaining general enough to capture the entire flow progress in a reasonable amount of calculation time.

# CHAPTER TWO

## LITERATURE REVIEW

An accurate representation of the effects of molding parameters on fluid profiles and pressure distributions in the RTM mold would greatly assist mold designers. Knowing the geometry of the fluid profiles with time would allow the mold designer to properly place the inlet ports and vent ports, which can dramatically enhance processing time as well as the quality of the finished part. Information about the pressure profile can be used to design the mold. RTM molds need not be made from traditional steel construction, but can be produced from lower cost composite.

Several processing variables have a major impact on the RTM process. These include the viscosity of the resin, the permeabilities of the reinforcement, the injection pressure or flow rate, and the mold geometry. The shapes which are generally produced with RTM are complex, and they have either constant pressure or constant velocity boundary conditions.. These and other complexities make analytical solutions nearly intractable, which accounts for the prevalence of numerical solutions in the literature.

## Viscosity

The resins used in RTM are usually viscous polymeric fluids. One approach to modeling this system is to assume a fluid which is Newtonian at the pressures and shear rates present [1,2]. This eliminates any complications which would arise due to non-Newtonian flow. The fluid is also modeled as incompressible. All non-Newtonian effects of the resin on the flow characteristics are generally neglected as these effects are not yet fully understood [1]. The viscosity of the resin can be measured with a cone and plate, or capillary rheometer; typically, uncatalized resin is used, as the addition of a catalyst does not significantly change the viscosity during the experimental time for resin impregnation [3]. The resin viscosity change during flow is either neglected, or modeled as a power law [4].

## Permeability

The permeability of the reinforcement is an important parameter to evaluate in order to properly model the flow in the RTM mold. The permeability of the reinforcement varies with direction and can be interpreted as the resistance of the fiber preform to the flow of resin. If the permeability is too low, then the pressure required to fill the mold becomes prohibitively high, or the fill time becomes long.

Many authors begin with Darcy's law, which is applicable to flow through porous media, as a basis for evaluation of the permeability parameters.

$$q_x = -\frac{k_x A}{\mu}\frac{\partial P}{\partial x}$$

$q_x$ is the flow rate in the $x$ direction

$k_x$ is the permeability in the $x$ direction

$A$ is the crossectional area for flow

$\mu$ is the viscosity of the resin

$\partial P/\partial x$ is the differential of pressure in the x direction

Chan and Hwang [5] evaluated the permeability from a theoretical treatment of the fibers as a series of parallel capillaries. Larson and Higdon [6] evaluated the permeability based on a theoretical treatment of the fibers arranged in a square array.

Another popular approach used by Bruschke and Advani [1], Coulter and Guceri [2,7], Gauvin and Chibani [3], Chang and Kikuchi [8], and Martin and Son [9], is to determine the permeabilities of a reinforcement fabric from experimental data. The procedure involves filling a rectangular mold with reinforcement and then measuring the flow rate of a fluid through the mold under a prescribed pressure drop. Another method for determining the principal permeabilities of a preform has been used by Bruschke and Advani [1], Young and Wu [10], and Adams et al. [11]. In their studies a layer of mat was placed in a mold, the resin was injected in the center of the mold, and the resulting elliptical flow front was measured. Equations have been developed [11] which allow estimation of the principal permeabilities and their ratio, from the principal axes of the ellipse.

Of the two main ways in which permeabilities have been studied, the use of a completely filled mold gives permeabilities in the fabric which is completely filled, and at steady state. The method of elliptical flow front allows measurement of the permeability as the reinforcement is filling. This method has an added advantage in that both the transverse and longitudinal permeabilities can be determined with one experiment. The use of a completely filled mold requires that the reinforcement be realigned in the other dirrection before the transverse permeability may be measured.

Permeability has been studied as a function of the reinforcement porosity by Gauvin, Chibani, and Lafontaine [12].

## Mathematical Models

A unified approach to modeling composite processing was undertaken by Dave [13], who derived the governing equations in terms of Darcy's law. The general approach was to substitute Darcy's law for the equation of motion in the mathematical analysis. This allows for the derivation of simple equations from the continuity equation for the system of interest. For the RTM process, these equations are fundamentally elliptical in nature, and require the specification of all boundary conditions. However, due to the resin flow front, at least one of these boundaries is constantly moving, and its shape is constantly changing. The movement of the boundary is treated with a quasi-equilibrium assumption, that at any time step there is an equilibrium of forces along the flow front. This boundary can also be treated with a condition of vanishing shear stress; however, a constant pressure condition is more widely accepted. There are also two different ways to handle the injection port. At that point on the boundary a constant velocity or a constant pressure condition can be specified.

The moving boundary condition, and the complexity of shapes typically produced with RTM, make the analytical solution intractable. There are some one-dimensional problems which can be solved analytically, but the two and three dimensional problems become increasingly complex. This system is therefore generally treated with numerical methods.

## Numerical Solutions

Much work has gone into developing numerical methods for simulating the RTM process. One such effort was conducted by Crochet, Davies, and Walters [14], who developed a numerical solving code by the name of POLYFLOW. This package is a two dimensional finite element routine which was originally designed for modeling thermoplastic molding; it has been modified by Martin and Son [9] for use with RTM systems. Martin and Son found good agreement between experimental studies and the corresponding simulations for flow front position and pressure profile. They also considered resin distribution channels and the effect of varying permeabilities.

Coulter and Guceri [2] simulated two dimensional resin impregnation with a boundary fitted coordinate system method. This effort resulted in a finite difference code by the name of TGIMPG. The boundary fitted coordinate system has the advantage of being able to fit the flow front closely, which helps eliminate the error generated at the flow front due to interpolation between the cells in either a finite difference or finite element solver routine. With this approach, however, the generation of the mesh becomes complex.

Finally, Trochu et al. [15] developed a three dimensional finite element solver for the express purpose of solving RTM problems. Their solving routine, called RTMFLOT, solves the Darcy's law equations to obtain a pressure profile. Reference [16] describes the package which consists of DATAFLOT, MESHFLOT, FLOT, VISIFLOT, and HEATFLOT. These are five separate programs for meshing, solving and visualizing the pressure profiles and flow fronts.

All of the previous models concentrate on the macroflow front; that is, the overall movement of the fluid front. They do not take into account the presence of individual bundles of fibers or the channels present between these bundles. This approach is particularly useful when working with permeabilities which are not associated with one particular phase, such as in random mat. Although random mat can have anisotropic permeability properties, it does not have well defined channels. Another class of material which has been successfully modeled with this approach are the woven materials, as they too do not have well defined channels, but have definite directional properties. These models may show deficiencies in treating the channeling caused by misaligned preforms [2, 17].

There are fewer models which concentrate on the aspects of microflow [6, 17, 18], or the flow between the bundles of fibers. This type of microflow model is very useful in determining a flow regime within the bundles, and it gives a good approximation for the permeabilities within the bundles. These models set a packing arrangement for the fibers, usually defined on a set geometric grid. This grid is always regular, and facilitates the mathematical solution of the flow problem. The microflow models tend to loose sight of the overall resin flow, and add prohibitive complexity to numerical solutions.

Both macroflow and microflow regimes contribute to the overall solution, and as a result both approaches to solving the problem are significant [2]. Chang and Kikuchi [8] used an approach which treated the two phases differently, treating the bundles with Darcy's law, and treating the channels with Stokes flow. They then used a finite element routine to bring this microflow view to bear in solving the macroflow front problem.

## Verification

The general approach to verification of these models is to construct a mold of the shape being simulated, and experimentally measure the flow front to determine if it corresponds to the numerically calculated flow front [1, 2, 4, 7, 8, 13, 17, 20-23]. The pressure profile is then correlated against a few discrete points at which a pressure tap can be placed in the experimental mold [2, 4, 5, 8, 17, 20, 21].

# CHAPTER THREE

# MATHEMATICS

## Microscale

The RTM process consists of flowing resin into preforms composed of previously assembled fiber mats. These mats contain strands at high fiber content alternating with large channels which allow passage of resin. The channels provide areas of low permeability for the distribution of the resin, and the large strands provide a high fiber content which increases the structural performance of the composite.

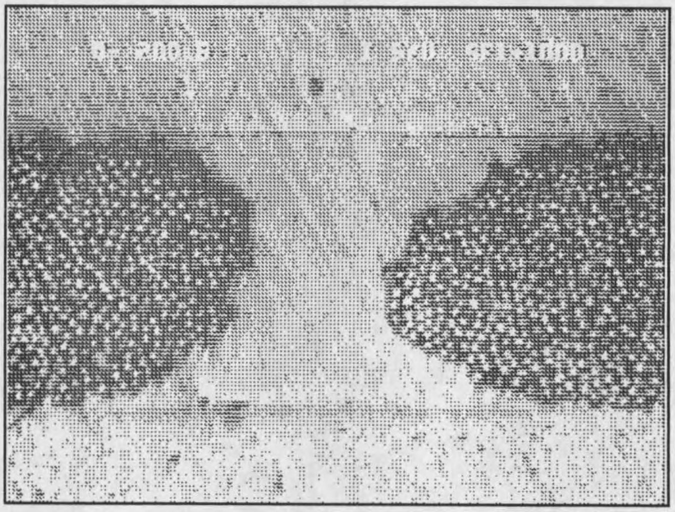

**Figure 1** Composite Cross-section.

The overall numerical model requires the determination of six permeabilities or effective permeabilities. These parameters describe the flow in the three principal directions in the strands, and the three principal directions in the channels. The flow in the strands can be described by application of Darcy's law, and is characterized by permeabilities in three directions. The permeability in the transverse direction within the strands is difficult to measure due to the difficulty of obtaining a constant packing arrangement independent of the pressure difference. The flow in the channels is treated with the application of laminar flow equations. These equations provide a velocity profile within the channels which can be used to directly relate the flow rate through a cell with the pressure difference across the cell. The ratio of these is used in the macroscopic model as an effective permeability in the channels.

A typical cross-section of the finished composite is shown in figure 1. This photograph shows the geometry of the resin channels. They consist mostly of I—shaped channels with elliptical sides. A finite difference solver routine has been used to approximate the laminar flow patterns inside of these channels. Since the flow in the channels is slow, the resin is usually very viscous and the diameters are small, it is expected that there will be little turbulent flow. Using a typical distance, D, of 415 $\mu$m, a fluid velocity, v, of 2 cm/s, a density, $\rho$, of 3.3 g/cm$^3$, and a viscosity, $\mu$, of 2 posies, the Reynolds number calculated [24] from $DV\rho/\mu$ is 0.1369, which is well within the laminar region. The flow of resin through the channel cross-section is calculated from classical channel flow equations.

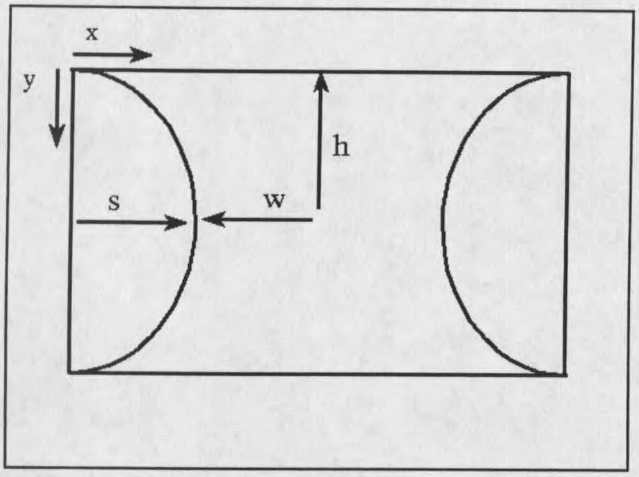


**Figure 2** Channel Cross-section.

In developing the basis for a mathematical model for the fluid flow in one unidirectional layer of fiber reinforcement, it is important to define the problem accurately. The cross-section of the channel in which the fluid flows is shown in figure 2. Several assumptions are made in the model.

First, it is assumed that the effects of gravity are negligible. This assumption is reasonable since, in most cases, the pressures which are applied to a unit volume of fluid are much greater than the weight of the fluid element. In most cases these channels are short in length. If a very long part were injected vertically, then gravity might have a significant effect, and would have to be taken into account.

Second, the velocity of the resin in the $x$ and $y$ directions is zero. Resin will not flow in the $x$ direction since it cannot flow through the walls of the mold. It will not flow in the $y$ direction because, as the resin enters the bundles, it becomes trapped at the flow front and subsequent flow does not displace the original fluid [25].

Third, the density of the resin is a constant in both time and space, as the resin is an incompressible fluid. If the resin changes density rapidly as it cures, this code will require modification.

The equation of continuity for this system in rectangular coordinates is given in equation 3.1. The density of the polyester resin is constant in space and time.

$$\rho\frac{\partial V_z}{\partial z}=0 \tag{3.1}$$

The equations of motion for this system are [26]

$$\begin{gathered}-\frac{\partial p}{\partial x}=0\\ -\frac{\partial p}{\partial y}=0\\ \rho\left(\frac{\partial V_z}{\partial t}+V_z\frac{\partial V_z}{\partial z}\right)=-\frac{\partial p}{\partial z}+\mu\left(\frac{\partial^2 V_z}{\partial x^2}+\frac{\partial^2 V_z}{\partial y^2}+\frac{\partial^2 V_z}{\partial z^2}\right)\end{gathered} \tag{3.2}$$

This assumes that viscosity is not a function of position, but that it is only a function of time. By using the equation of continuity, the equation of motion can be further simplified to the following

$$\rho\left(\frac{\partial V_z}{\partial t}\right)=-\frac{\partial p}{\partial z}+\mu\left(\frac{\partial^2 V_z}{\partial x^2}+\frac{\partial^2 V_z}{\partial y^2}\right) \tag{3.3}$$

The location of the sides of the ellipse will be found from

w

$$x=\sqrt{a^2-\frac{a^2(y-h)^2}{b^2}} \tag{3.4}$$

here (a) is the $x$ radius and (b) is the $y$ radius; (h) is half the height of the channel. Discretizing the differential equation yields

$$\rho\frac{(V_{z(t+1)}-V_z)}{\Delta T}=-\frac{\Delta P}{\Delta z}+\mu\left(\frac{V_{z(x-1)}-2V_z+V_{z(x+1)}}{(\Delta x)^2}+\frac{V_{z(y-1)}-2V_z+V_{z(y+1)}}{(\Delta y)^2}\right) \tag{3.5}$$

As the system is considered at equilibrium, the time derivative drops out, and what is left is

$$\frac{\Delta P}{\Delta z}=\mu\left(\frac{V_{z(x-1)}-2V_z+V_{z(x+1)}}{(\Delta x)^2}+\frac{V_{z(y-1)}-2V_z+V_{z(y+1)}}{(\Delta y)^2}\right) \tag{3.6}$$

The channel in figure 1 is meshed in the $x$ and $y$ directions and eq.3.6 is used to solve for the velocity distribution given the change in pressure along the $z$ direction

$$\frac{\Delta P}{\mu\Delta z}=\frac{V_{z(x-1)}}{(\Delta x)^2}-\frac{2V_z}{(\Delta x)^2}+\frac{V_{z(x+1)}}{(\Delta x)^2}+\frac{V_{z(y-1)}}{(\Delta y)^2}+\frac{2V_z}{(\Delta y)^2}+\frac{V_{z(y+1)}}{(\Delta y)^2} \tag{3.7}$$

This final equation, 3.7, provides the coefficients of the variables in the system of linear equations. The solution to this system of linear equations provides a relationship between the pressure drop through the channels and the velocity of the resin within the channels. Given a pressure drop, the velocity profile can be obtained. This system of equations can be solved most easily in matrix form.

$$[A]=[V_z][Q] \tag{3.8}$$

$$\left[\begin{matrix} \left(-\frac{2}{(\Delta x)^2}-\frac{2}{(\Delta y)^2}\right) & \frac{1}{(\Delta x)^2} & 0 & 0 & \frac{1}{(\Delta y)^2} & 0 & 0 & 0 & 0 \\ \frac{1}{(\Delta x)^2} & \left(-\frac{2}{(\Delta x)^2}-\frac{2}{(\Delta y)^2}\right) & \frac{1}{(\Delta X)^2} & 0 & 0 & \frac{1}{(\Delta Y)^2} & 0 & 0 & 0 \\ 0 & \frac{1}{(\Delta x)^2} & \left(-\frac{2}{(\Delta x)^2}-\frac{2}{(\Delta y)^2}\right) & \frac{1}{(\Delta X)^2} & 0 & 0 & \frac{1}{(\Delta Y)^2} & 0 & 0 \\ 0 & 0 & \frac{1}{(\Delta x)^2} & \left(-\frac{2}{(\Delta x)^2}-\frac{2}{(\Delta y)^2}\right) & \frac{1}{(\Delta x)^2} & 0 & 0 & \frac{1}{(\Delta y)^2} & 0 \\ \frac{1}{(\Delta y)^2} & 0 & 0 & \frac{1}{(\Delta x)^2} & \left(-\frac{2}{(\Delta x)^2}-\frac{2}{(\Delta y)^2}\right) & \frac{1}{(\Delta x)^2} & 0 & 0 & \frac{1}{(\Delta y)^2} \\ 0 & \frac{1}{(\Delta y)^2} & 0 & 0 & \frac{1}{(\Delta x)^2} & \left(-\frac{2}{(\Delta x)^2}-\frac{2}{(\Delta y)^2}\right) & \frac{1}{(\Delta x)^2} & 0 & 0 \end{matrix}\right]_{ETC} \qquad \textbf{(3.9)}$$

The pressure drop and the length are already known, so the solution only requires arranging the resulting equations into a five-diagonal matrix, inverting the matrix, and multiplying the resulting matrix by the solution vector. A typical grid would produce a [Q] matrix like that shown in equation 3.9.

For a 10x10 grid the resulting matrix would have 100 rows and 100 columns. This matrix can then be inverted and multiplied by the left-hand-side vector [A] to produce the solution vector [$V_z$]. The left hand side vector [A] contains a column of values which are

$$\frac{\Delta P}{\mu \Delta z}$$

The solution vector [$V_z$] will contain the steady state velocity of the fluid in that particular cross-section. The average velocity in the entire channel is then calculated by multiplying each velocity component by the cross section over which it acts, and then dividing that product by the total area of all the cross sections. This average velocity is then used in Darcy's law for one dimensional flow to arrive at a permeability for the channel. Darcy's law for one dimensional flow is

$$V_z = -\frac{k_z}{\mu}\frac{\Delta P}{\Delta z} \qquad \textbf{(3.10)}$$

Using this equation, a value for $k_z$ can be back calculated. This value is the equivalent permeability of the channel in the $z$ direction. The equivalent permeabilities of the channels in the other two directions can also be calculated in this way, using their respective geometries. These two directions are not expected to be significant in single layers due to the presence of bundles on either side, and the presence of mold faces on the top and bottom. However, in large stacking arrangements, these permeabilities couple the resin in the channels in different layers, and thus are important in the overall model.

The above analysis gives permeabilities in the three principal directions inside the channel areas. This leaves the permeabilities in the bundle areas to be considered. The permeability in the longitudinal direction can easily be measured as described in Chapter 4 (Parameter Measurement); the permeabilities in the transverse directions in the bundles are not so easily measured, and must be obtained separately as described later.

## Macroscopic System

The macroscopic system which contains the layers of reinforcement, the mold faces, the injection and vent ports, and the resin is considered next. The reinforcement layers use a different coordinate system than that used by the individual cells. The individual cells use an $x$, $y$, $z$ coordinate system, relative to the boundaries of the cells. The reinforcement layers use an $x_2$, $x_1$, $x_3$ coordinate system, where, $x_2$ is transverse to the strands, $x_1$ is parallel to the strands, and $x_3$ is through the thickness of the part. For stranded reinforcements $x = x_2$ $y = x_1$ and $z = x_3$. Each layer of reinforcement in the model uses its own coordinate system, with the $x_1$ direction always parallel to the strand direction. All layers share the same $x_3$ or through the thickness coordinate, and the same origin. The different coordinate systems allow the permeabilities in the principal directions of the reinforcement to be applied directly to the difference cells, with no modification. The $x_3$ coordinate commonality allows for the communication of resin flow between the individual layers.

Darcy's law is used to model the flow within the fiber mats, but first the pressure profile within the mats must be known. If the system is at equilibrium, then the pressure profile can be calculated from the equation of continuity for this system. Substituting Darcy's law (eq. 3.10) for the velocity terms, equation 3.11 results

$$\frac{\rho}{\mu}\left(\frac{\partial^2 K_{x_1} P}{\partial x_1^2}+\frac{\partial^2 K_{x_2} P}{\partial x_2^2}+\frac{\partial^2 K_{x_3} P}{\partial x_3^2}\right)=0 \tag{3.11}$$

This is an elliptical equation and can be solved at equilibrium, given the boundary conditions. This equation is then discretized over the domain of the reinforcement.

Equation 3.11 is discretized on the following grids for the $x_1$, $x_2$, and $x_3$ directions. The $x_1$ direction is along the length of the strands, the $x_2$

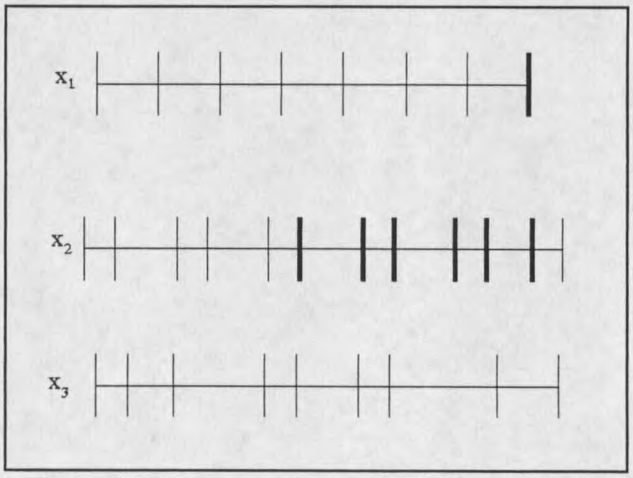


**Figure 3** Macro Flow Grid Definitions for the Spacial Directions.

direction is transverse to the strands, and the $x_3$ direction is in the thickness direction of the part. The $x_2$ direction consists of a series of alternating equal width cells, the $x_1$ direction consists of a series of equal length cells, and the $x_3$ direction consists of a series of unequal height cells. Using Taylor series expansions for the approximations for the three partial derivatives in equation 3.11 on the grids in figure 3 results in an implicit approximation scheme shown below.

$$
\begin{gathered}
K_{x_2}^{*}\left(\frac{p_{i-1}-2P_i+P_{i+2}}{(\Delta x_2^{*})^2}\right)+K_{x_1}^{*}\left(\frac{P_{j-1}-2P_j+P_{j+1}}{(\Delta x_1)^2}\right)+\frac{1}{\mu}\left(\frac{K_{k-1}P_{k-1}-(K_{k-1}+AK_{k+1}P_k+AK_{k+1}P_{k+1}}{(\Delta x_3^{*})^2}\right)=0 \\
\Delta x_2^{*}=\frac{(\Delta x_{2,1}+\Delta x_{2,2})}{2},\quad (\Delta x_3^{*})^2=\frac{(\Delta x_{3,k}+\Delta x_{3,k-1})^2}{8}+\frac{A(\Delta x_{3,k}+\Delta x_{3,k+1})^2}{8} \\
A=\frac{K_{k-1}}{K_{k+1}}\frac{(\Delta x_{3,k}+\Delta x_{3,k-1})}{(\Delta x_{3,k}+\Delta x_{3,k+1})}
\end{gathered}
\tag{3.12}
$$

where $K_{x1}^{*}$, and $K_{x2}^{*}$ are the permeabilities in the individual directions divided by the viscosity. This difference scheme is an approximation to the original equation to the order $(\Delta x_1)^2$, $(\Delta x_2)^2$, and $(\Delta x_3)^1$.

Equation 3.12 can then be solved in the same way that the previous difference scheme was solved; that is, by writing an equation for each of the cells, and including the permeability terms of the bordering cells, then inverting the coefficient matrix and solving for the solution vector. This method of solving for the pressures at each of the nodes would work and be the most accurate. However, these systems of nodes usually run in the tens of thousands of elements, and large moldings could conceivably run much higher. In sets of linear equations of this magnitude the time of solving by this method becomes unmanageable. Instead, an iterative relaxation method was used.

In this method (called the Gauss-Seidel method [27]), the difference equation is solved for the pressure present at the central cell. Then this equation is applied to all of the cells, and the pressure of the central cell is calculated. Once all of the cells have been calculated once, the procedure repeats. With enough iterations, the system of cells approaches the same solution which one would obtain by inverting the matrix each time. There is a trade off in accuracy and time; matrix inversion introduces machine error, and it is costly in terms of the additional time required for more cells. The relaxation methods can achieve highly accurate solutions, however they converge rather slowly. One must determine if the time required to invert the matrix is more than the time required to relax the solution to within an acceptable tolerance. The pressure profile must be solved at the beginning of each time step, and this is clearly not feasible with a matrix inversion routine. Here is where the iterative method is most effective. As the resin flows through the cells, the pressure profile evolves from the previous pressure profiles. If the start of the iteration for the current profile is set to the profile at the end of the previous time step, then the iteration scheme only has to make up for the addition of current flow. If the time steps are small, then the pressure profiles at subsequent time steps differ little from those at the previous ones, and the relaxation method converges rapidly to the new pressure profile. This routine reduces the time required for the resulting algorithm to $O(n)^2$ instead of $O(n)^3$, in most cases [27].

# CHAPTER FOUR

# PARAMETER EVALUATION

There are several parameters inherent in the model which must be determined. These parameters are the viscosity of the resin, the geometric parameters, and the permeability parameters.

## Viscosity

The viscosity of the resin was measured using a capillary rheometer (figure 4). It consists of a small capillary of known diameter connected to a large precision milled piston. The piston chamber is filled with the resin, and a weight is applied to the piston. From the force applied on the piston, the length and diameter of the capillary, and the flow rate

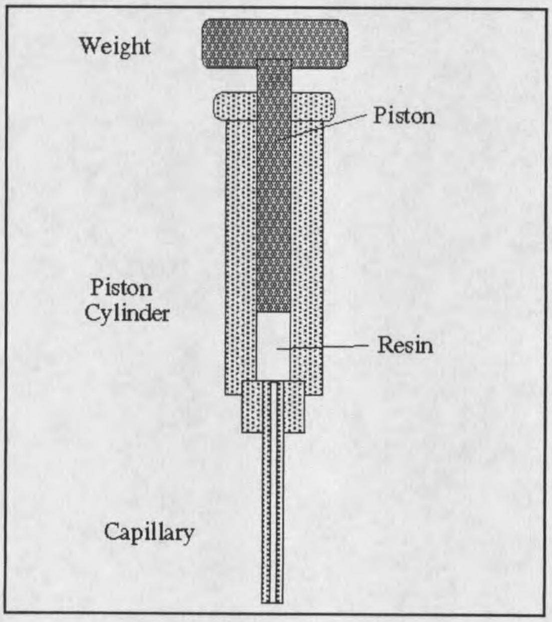


**Figure 4** Capillary Rheometer.

of the resin, a viscosity can be calculated. This rheometer was fabricated by Hedley [25] according to ASTM standard D 3835-90 [28], and the viscosity of the resin is calculated using equations supplied with the standard.

## Geometric

The geometric parameters relate to the geometry of the mold and the architecture of the reinforcement. The geometry of the mold is in this case a flat rectangular plate. This geometry is hard coded into the mesh generator, and is a sum of the numbers and arrangements of the cells included in the solution set. These parameters are the length and width of the mold. The third dimension, the height, is not given explicitly, but it is a result of the sum of the heights of the individual layers.

The geometric parameters which relate to the architecture of the fabric in the individual layers can most easily be evaluated by producing a molding prototype, and measuring the distances under a microscope. The architecture of the reinforcement is dependent largely on fiber volume fraction. If the geometric parameters of the reinforcement are measured at several fiber contents, then that data can be applied to all future simulations without having to evaluate each case individually.

The fiber architecture parameters are the length, width and height of the channels and strands in the reinforcement. The length is largely an arbitrary parameter as it has little actual physical significance. The fiber strands and channels generally run the entire length of the mold, and thus have no convenient breaking points. It is

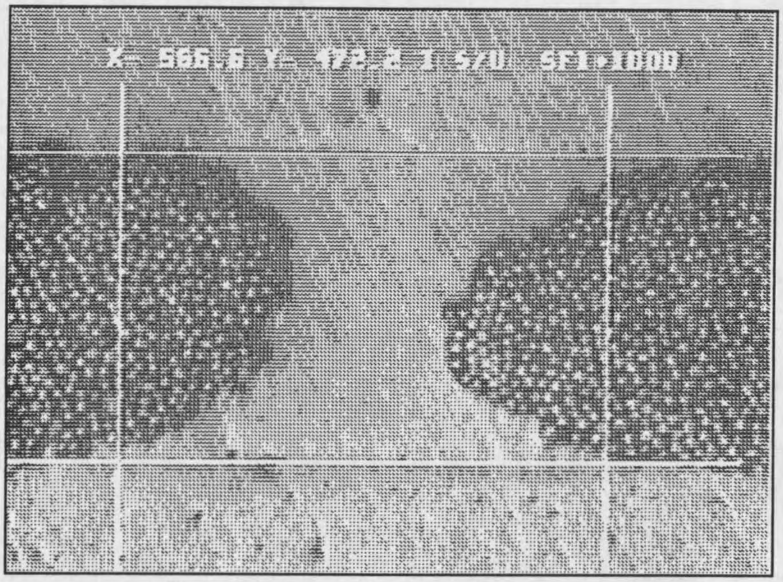


Channel Cross-section.

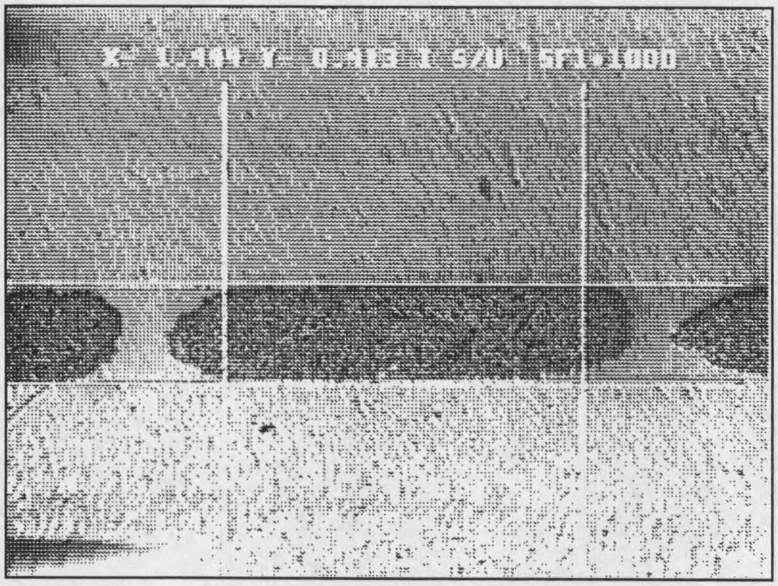

Strand Cross section.

**Figure 5** Measurements of Channel Geometries important, however, to keep this length comparable to the other two dimensions to maintain a consistent cell aspect ratio. If the length is too long, the error associated with calculating the pressure profile at the flow front will become significant.

Other parameters can be easily measured under a microscope. Figure 5 shows photographs which were used to measure these parameters. In layers where there is no channel architecture, random mat for instance, this approach makes little sense. In these layers a better approach would be to assign a grid spacing similar to those in adjacent layers. This allows for adequate vertical connections between the layers, and does not compromise the random mat layer.

## Permeability

The permeabilities of the layers must also be either measured or approximated. First, the permeabilities of the channels are approximated from classical channel flow theory, which is described in Chapter 3.

The permeabilities of the bundles must then be either measured or approximated. The first approach was used to obtain a measurement of the bundle permeability in the axial, $x_1$ direction. Figure 6 shows a device that can be used to measure permeabilities. It consists of a large reservoir which can be pressurized by application of high pressure air at the inlet. This reservoir is attached to a tube which is packed with the reinforcement. Because the attempt was to pack these fibers as closely as possible to the arrangement seen in the bundles in actual reinforcement, all of the binder thread which is used to hold the fabric together was removed. The reinforcement fibers were then aligned, and packed into the tube in anywhere from 50% to 66% fiber volume fraction arrangements. At the lower end of the tube, is a metal grid to prevent the fibers from being washed out of the tube.

In operation, resin is placed in the reservoir and air pressure is applied. It is

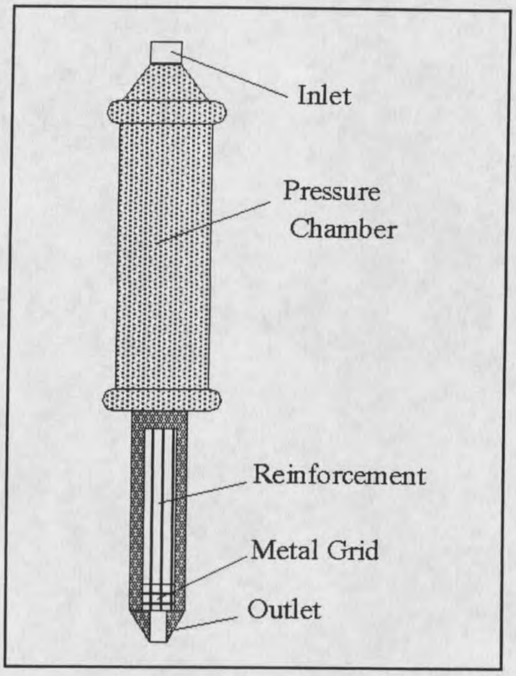


**Figure 6** Permeate Meter.

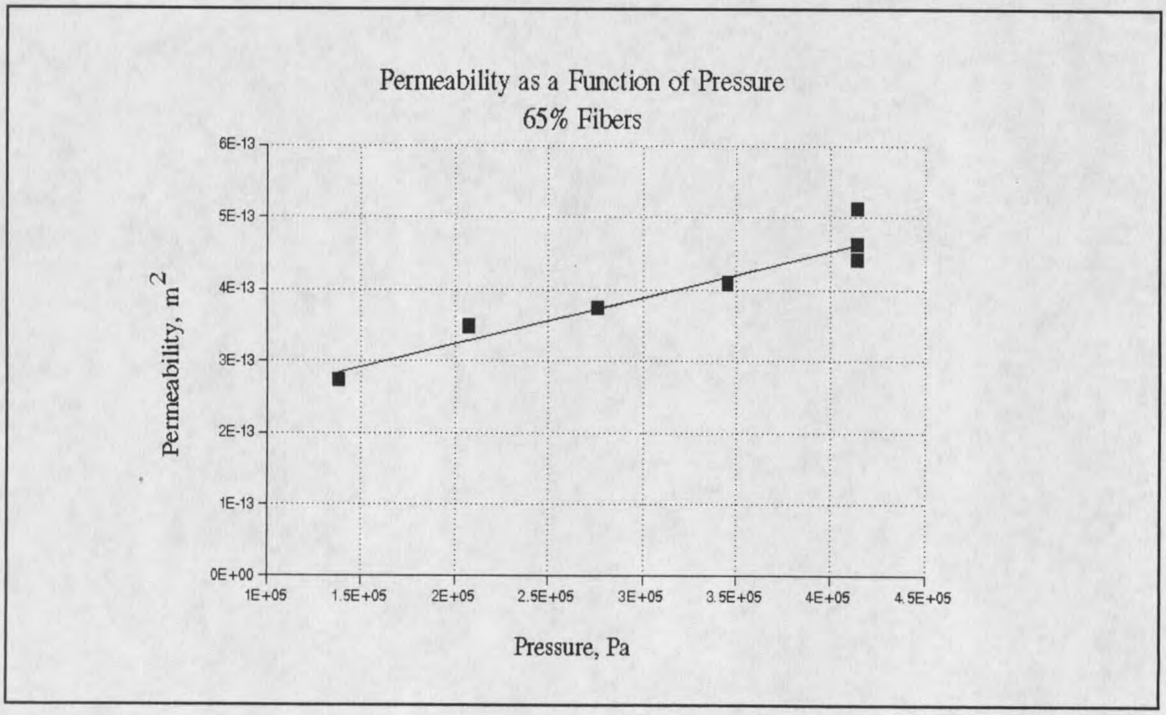


**Figure 7** Permeability as a Function of Pressure.

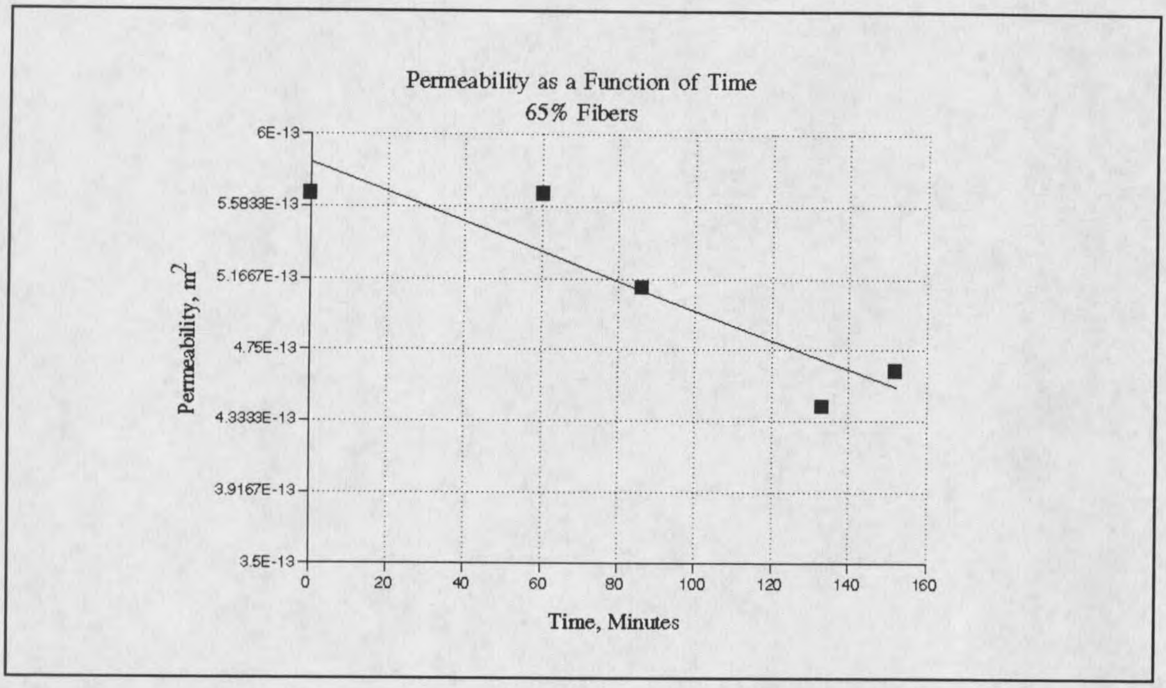


**Figure 8** Permeability as a Function of Time.

necessary to wait for a period of time for the reinforcement to become fully saturated, and the resin stream to run free of porosity. Then, varying pressures are applied to the reservoir, and the flow rate of the resulting stream of resin is measured. This is done by measuring the time required for a specific amount of resin to flow through the reinforcement. Applying Darcy's law (eq. 3.10), a permeability can be calculated. Figure 7 shows the resulting data. The permeability is shown to increase slightly with increasing pressure. This behavior is not consistent with theory, but it was observed by Martin and Son [9], Leek et al. [29] and Hedley [25] in fabrics. It is thought to be the result of pressure effects on packing efficiency. Similar data for other fiber contents are given in Appendix A.

The data was also correlated with time, and figure 8 shows that there is a negative correlation between the total length of time that the resin has been flowing through the fibers and the permeability of the fiber plug. Two possibilities for this behavior present themselves. First, the styrene could be evaporating from the resin (Chapter 5), producing a resin which is more viscous as the process proceeds. Second, the resin could be contaminated, and the contaminants could be plugging up the pores between the fibers in the reinforcement. In an attempt to determine if there was a change in viscosity over time, the viscosity of the resin was tested after each permeability test. The results showed that the viscosity of the resin did not change significantly over the course of the experiment (Appendix A).

In order to determine if there was some foreign material in the resin that could be causing problems, a sample was taken to Parker Filtration for analysis. They did find some debris in the resin which could interfere with flow through the bundles, as described in Appendix A.

The final parameter to determine is the radial ($x_2$ direction) permeability in the bundles. As this parameter is difficult to measure due to the shape of the bundles, an attempt was made to calculate this from the Kozeny-Carman equation [24].

$$\frac{\Delta p G_c \Phi_s^2 D_p^2 \eta^3}{L V_0 \mu (1-\eta)^2} = 150 \qquad \textbf{(4.1)}$$

where $\Delta p$ is the pressure drop, $G_c$ is the Newton's law proportionality factor, $\Phi$ is the sphericity, $\varepsilon$ is the porosity, L is the total bed depth, $V_0$ is the velocity of the resin, and $\mu$ is the viscosity of the resin. Rearranging this equation into the form of Darcy's law, and supplying all of the relevant information should result in a theoretical permeability. Rearranging and evaluating the equation with a sphericity of 0.192, an equivalent diameter of 3.124e-4 m, and a porosity of 35%, yields eq. (4.2)

$$\frac{\Phi^2 D^2}{150(1-\epsilon)^2} = \frac{Q\mu L}{\Delta P A} = 5.68x10^{-11} m^2 \tag{4.2}$$

Since this equation was generated for the case of roughly spherical packing, it is expected that the value obtained will not be particularly accurate. However, it will provide a starting point with which to begin testing the model. A unidirectional single layer simulation is evaluated, in which this is the only adjustable parameter. Matching this simulation to the experimental results provides an improved value for this parameter.

# CHAPTER FIVE

# EXPERIMENTAL

## Materials

The reinforcements used in this study were manufactured by Knytex, and generally consisted of stranded structures. The fabrics under study were the D155, (figure 9), and the DB240 (figure 10).

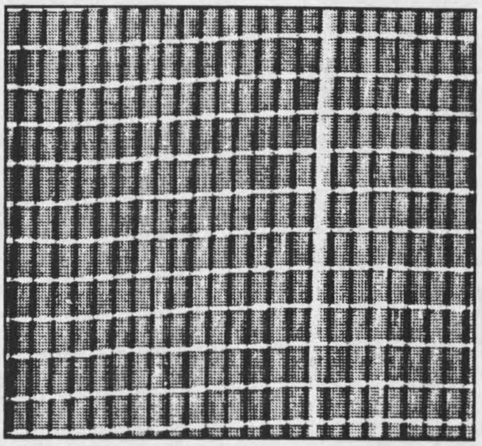

**Figure 9** D155 Fabric.

The D155 material is a unidirectionally oriented continuous strand mat with a weight of 480g/m (15.5 oz/yd). This mat can be easily cut and arranged in a mold in the directions needed for strength. The DB240 material consists of two layers of unidirectional material stitched together with polyester thread. The two layers in this fabric are oriented at plus and minus forty-five degrees to the normal fabric direction. The combination of D155 and DB240 simulates a triax fabric which has fibers at zero, +45 and -45 degrees to the normal fabric direction.

An orthophthalic polyester resin (COR63-AX-051, BATCH# 1195267), manufactured by Interplastic Corporation, was used for all experiments. The resin consists of polyester with styrene added as a solvent and cross linking agent. Methyl Ethyl Ketone Peroxide (MEKP) was used as a catalyst. This resin has a cure time of 25 minutes at 25 °C (77 °F) when catalyzed with 3% MEKP. No degassing was performed on the resin before injection in any of the experiments.

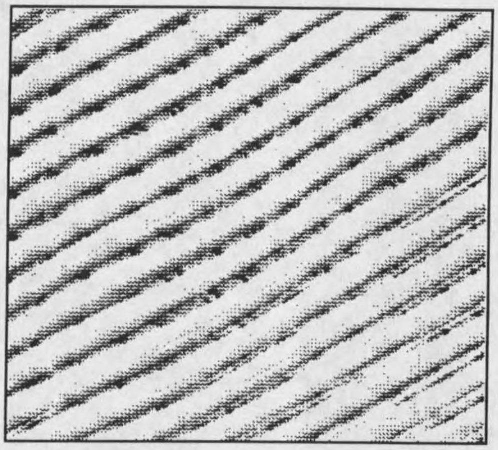

**Figure 10** DB240 fabric.

Mold Release (A1000) sold by CAMIE was used to coat the surface of both the aluminum plate and the glass mold face.

Equipment

The resin delivery system for high pressure trials consisted of a pressure vessel which could be filled with compressed air (figure 11). For low pressure runs (less than 13800 pa (20 psi)), a smaller reservoir was used. This reservoir allowed for more accurate

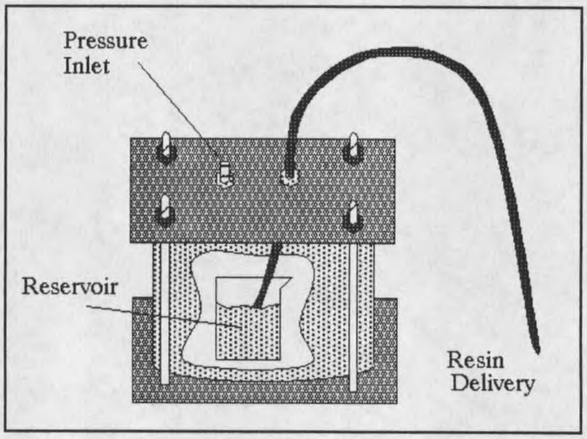


**Figure 11** High Pressure Resin Delivery System (1 liter Reservoir).

control of the pressure, and was more manageable where small amounts of resin were required. In both cases the catalyst was added to the resin before it was placed in the reservoir for delivery.

An RTV silicone gasket was used to seal the mold cavity. This material is chemically inert to the resin and the curing agent, and it provides a flexible seal. Since the gasket can be compressed, it allows for greater variability in the thickness of parts which could be produced from this one mold, as compared with a rigid gasket.

A micrometer was used to ensure that the thickness of the plate was uniform throughout the length and width of the mold within a tolerance of 0.1 mm. A flat piece of aluminum was placed on top of the tempered glass to protect it from the C-clamps which were used to hold the glass in place. The injection port was located in the center of the width of the aluminum plate, about one half inch in from the left most edge. The vent ports were located on the right hand edge, approximately one half inch in from the corners.

The resin delivery system was connected to the mold (figure 12), which consisted of a 13.2mm thick polished aluminum base plate, and a 12.3 mm thick tempered glass top plate, separated by the silicone gasket. A series of clamps were used to control the thickness of the

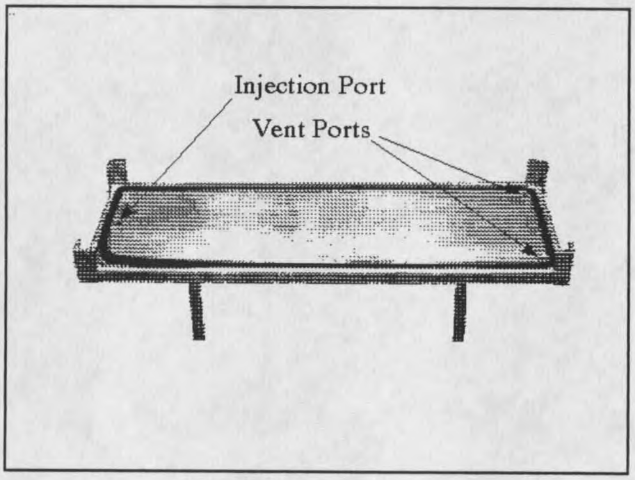


**Figure 12** Experimental Mold.

mold cavity. The interior of the mold measured 146 mm by 432 mm. A channel was milled in the aluminum base plate to hold the gasket.

The pressure at the injection port was recorded with a transducer (OMEGA PX26-030GV) which was connected through a T-junction in the injection line. The junction was placed approximately one inch from the injection port, and the transducer was buffered from the resin with four inches of tubing filled with corn oil. This was necessary to protect the transducer from contact with the resin as resin would damage the transducer. Additionally, if the resin were to cure while inside of the transducer, subsequent readings would not be accurate. This transducer mechanism could not be used at pressures of greater than thirty psi, so for the high pressure experiments, the pressure was read from a gage on the high pressure resin delivery system, measuring the air pressure applied to the resin.

A video camera was positioned above the mold to record the position of the flow front with time. A digital camera was also positioned over the mold. The flow positions recorded with this camera could then be used to correlate with the model.

## Single layers

As mentioned in chapter 4, the first trial was a single layer of unidirectional material, which was used to measure the transverse permeability of the bundles. In this case the effect of the longitudinal permeabilities can be isolated from that of the transverse permeabilities. The best place to measure the transverse permeabilities is adjacent to the injection port. Special care had to be taken to prevent any channeling along the sides of the mold. The reinforcement was cut exactly to fit. The gasket used in this case was one layer of double sided mounting tape (ScotchTM Cat. #110). It was necessary to switch to this type of seal to allow the mold to reach a thickness of one layer. The presence of the tape also reduced the interior cavity of the mold to 121 mm x 406 mm. The tape expands slightly as the mold is closed. This expansion ensured that no resin could escape around the cut ends of the bundles.

The transverse permeability of the channels is expected to be much greater than that of the strands, and is not expected to interfere with the measurement. An inlet pressure of 137,000 Pa (20 psi) was used for these experiments.

## Multi-Layers

Three multi-layer experiments were conducted; in all cases, the resin was injected at 34500 Pa (50 psi). The first consisted of two layers of D155 fabric. These were placed in the mold at ±45 degree angles. The mold was sealed with tape.

The second multi-layer experiment consisted of three layers of D155 fabric oriented at +45, 0 and -45 degree angles. The RTV gasket was used in this and the next experiment.

In the third multi-layer experiment, two layers of fabric were used. One layer of D155 fabric was used for the unidirectional layer, and one layer of DB240 fabric was used for the ±45 plies. The final fiber orientation was 0, ±45 degrees.

| Test Description | Number of Replicates | Motivation | Results to be Obtained |
| --- | --- | --- | --- |
| Single Layer (0) | 1 | Transverse Strand Permeabilities | Flow Front Positions Especially in $x_2$ Direction |
| Tripple Layer (+45/0/-45) | 2 | Inter Layer $x_3$ dirrection interactions | Flow Front Positions in Topmost ,+45, Layer |
| Forty-Five Layer (±45) | 1 | Square flow Front Geometry | Shape of Flow Front, and Location in Time |
| Fourth Laminate (0/±45) | 1 | Interactions Between Two Different Types of Fabric | Shape and Position of Flow front with Time |

**Table 1** Test Matrix

# CHAPTER SIX

# RESULTS

## Single Layers

Figure 13 shows experimental data for the position of the flow front within the mold with time for the single 0° layer trials. Figure 14 shows the calculated position of the flow front for the same conditions. The parameters used in the numerical approximation are shown in Table 2. Note that the subscripts 1, 2, 3 refer to the fabric directions for a particular layer parallel to the fibers, perpendicular to the fibers, and in the thickness direction, respectively.

Channel permeabilities were calculated from the channel geometries as described earlier. The strand axial permeability was measured, while the strand radial permeability was varied in several simulations in order to arrive at a value which would closely approximate the width direction position of the flow front (Appendix A). The injection pressure was ramped up to 138,000 Pa (20 psi) in one second, and then held steady at that level for the duration of the simulation.

| | | | |
|---|---|---|---|
| Part Geometry | | Viscosity | 1.17 Poise |
| length | 406.4 mm | Time Step | 0.5 second |
| width | 60.33 mm | Pressure Sensitivity | 1 Pa |
| Bundle Geometry | | Channel Geometry | |
| length | 5.000 mm | width | 0.567 mm |
| width | 1.444 mm | center width | 0.166 mm |
| height | 0.473 mm | height | 0.473 mm |
| Bundle Permeabilities | | Channel Permeabilities | |
| $kx_1$ | 1.0e-12 $m^2$ | $kx_1$ | 3.1e-10 $m^2$ |
| $kx_2$ | 5.2e-13 $m^2$ | $kx_2$ | 2.0e-10 $m^2$ |
| $kx_3$ | 5.2e-13 $m^2$ | $kx_3$ | 2.0e-10 $m^2$ |

**Table 2** Parameters Used for the Single Layer Simulation

When determining the experimental position of the flow front with time, a line is hand drawn around the flow front contour on a photograph taken through the glass face of the mold. For purposes of direct comparison, a predicted flow front position is superimposed on the photograph of the flow front at 10 minutes in figure 15. The predicted flow front gives good agreement with the actual flow front. At around 10 minutes injection time, the resin began to flow further ahead inside the strands than in the channels between the strands. This behavior was explained as capillary flow in the strands and is due to surface tension along the resin-fiber interface. This type of flow is not yet included in the model.

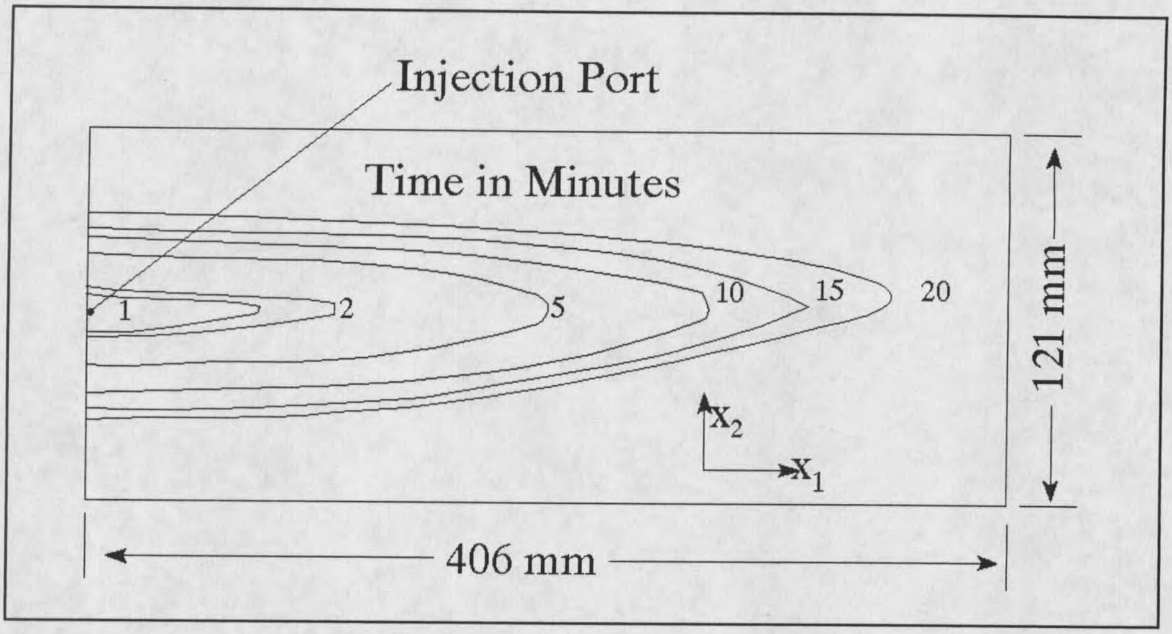


**Figure 13** Single Layer Experimental Flow Front Position with Time.

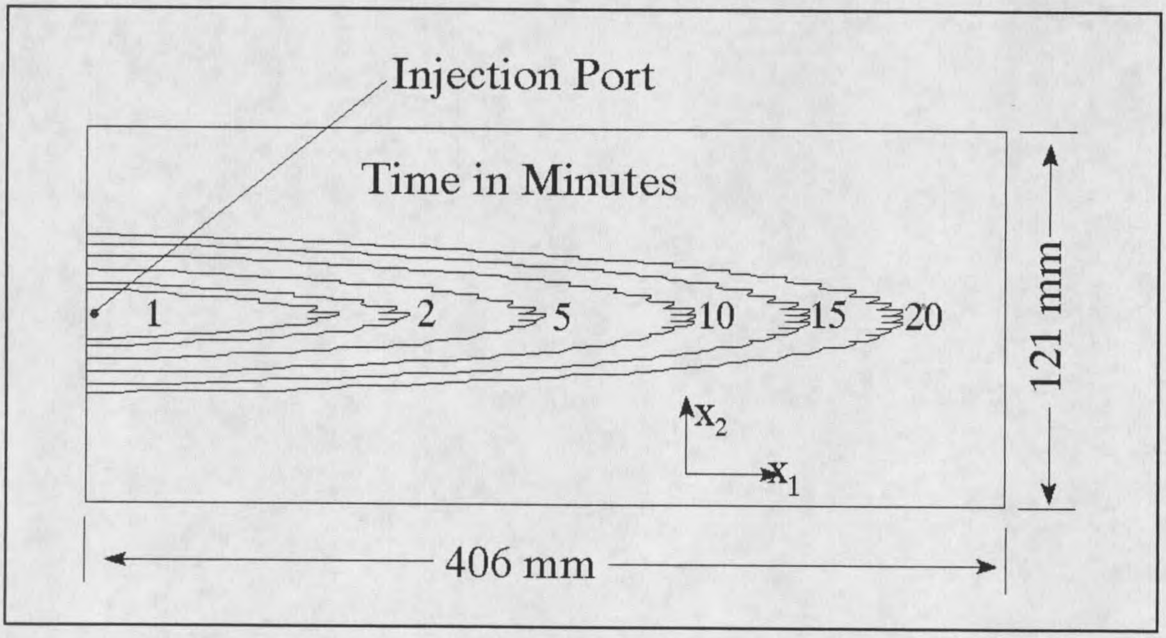


**Figure 14** Single Layer Calculated Flow Front Position with Time.

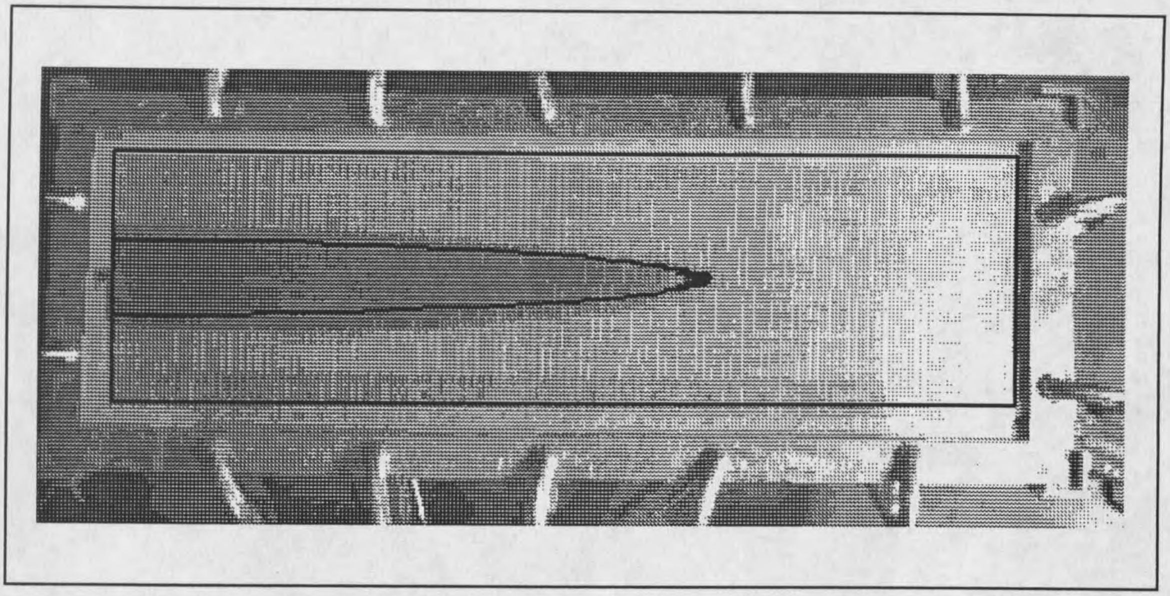

**Figure 15** Single Layer Experimental (Photograph) and Simulated (Line) Flow Front at 10 min.

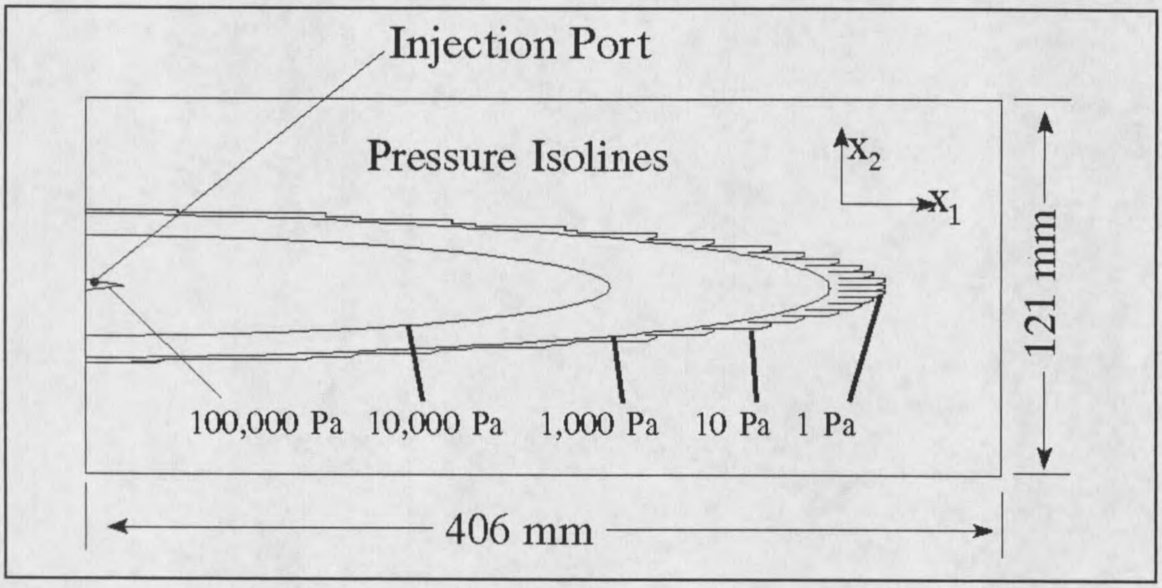


**Figure 16** Calculated Pressure Profile, Single 0° Layer at 20 min.

The model also calculates the pressure profile on a per-layer basis. For the final time step, where the pressure is the highest, the profile is shown as a series of